ISSN 0021-8944, Journal of Applied Mechanics and Technical Physics, 2017, Vol. 58, No. 2, pp. 232–243. © Pleiades Publishing, Ltd., 2017.
Original Russian Text © M. Daba, P. Devaraj.

UNSTEADY DOUBLE DIFFUSIVE MIXED CONVECTION FLOW OVER A VERTICALLY STRETCHING SHEET IN THE PRESENCE OF SUCTION/INJECTION

M. Daba and P. Devaraj[a]

UDC 536.2:532.5

Abstract: An unsteady double diffusive mixed convection boundary layer flow over a vertically stretching sheet in the presence of suction/injection is investigated in this paper. The governing partial differential equations are reduced by applying suitable transformations to a set of nonlinear ordinary differential equations, which is solved by the Keller box method. The influence of various flow parameters on the velocity, temperature, and species concentration profiles of the fluid is studied. The effect of some problem parameters on the skin friction coefficient in the presence of suction/injection is considered.

Keywords: mixed convection, suction/injection, stretching sheet, buoyancy force.

DOI: 10.1134/S0021894417020067

INTRODUCTION

When the flow is driven by buoyancy forces due to temperature and concentration gradients simultaneously, it is called a double diffusive mixed convection flow. One of the examples is the flow in an ocean, where heat and salt concentrations exist with different gradients and diffuse at different rates. Such flows also occur in various scientific and technological fields like astrophysics, biology, geology, chemical processes, etc. [1].

A laminar boundary layer flow of a fluid over a flat plate was first studied by Blasius [2], and this work was extended by Sakiadis [3] for the case of a moving plate in a quiescent fluid. Cortell [4] examined the Blasius flat plate flow problem in the presence of thermal radiation. Cortell [5] also extended his work to study the effect of thermal radiation for a moving plate in a quiescent fluid under convective surface boundary conditions. A mixed convection flow over a moving vertical plate due to the effect of thermal and mass diffusion was studied by Patil et al. [6]. They solved the problem numerically using an implicit finite difference scheme in line with quasi-linearization. Aydin [7] analyzed a steady laminar boundary layer flow over a porous flat plate with suction/injection imposed at the wall. A variable thermal conductivity and heat transfer problem of a boundary layer flow past a stretching plate was studied by Ahmad et al. [8]. A problem of a mixed convection boundary layer flow over a vertical plate with velocity and temperature slip was investigated by Bhattacharyya et al. [9]. A magnetohydrodynamic (MHD) mixed convection flow with the effects of the Ohmic heating and viscous dissipation was examined by Aydin [10]. Pop and Na [11] analyzed a boundary layer flow over a permeable stretching sheet in the presence of a magnetic field. Further, Bakar et al. [12] investigated a steady laminar flow over a stretching sheet with a convective boundary condition and partial slip. Chiam [13] scrutinized the boundary layer flow and heat transfer in a fluid with a variable thermal conductivity over a linearly stretching sheet. Heat transfer characteristics of a stretching surface with a variable

Department of Mathematics, College of Natural Sciences, Jimma University, Jimma-378, Ethiopia; mitbru2007@yahoo.com. [a] Department of Mathematics, College of Engineering Guindy, Department of Mathematics, Anna University Chennai, India, PIN 600025; devaraj@annauniv.edu. Translated from Prikladnaya Mekhanika i Tekhnicheskaya Fizika, Vol. 58, No. 2, pp. 53–65, March–April, 2017. Original article submitted September 10, 2014; revision submitted August 10, 2015.

temperature were studied analytically by Grubka and Bobba [14]. Recently, Ali et al. [15] studied the problem of a steady laminar MHD mixed convection stagnation-point flow of an incompressible viscous fluid over a vertical stretching sheet.

An unsteady free convection boundary layer flow over a moving vertical surface was studied by Kumari et al. [16]. A similar case for a stretching vertical surface in a quiescent fluid was considered by Ishak et al. [17], and that for a continuously moving vertical plate was studied by Anilkumar [18]. Convection for an impulsively stretched permeable vertical surface in an unbounded quiescent fluid in the presence of a transverse magnetic field was investigated by Kumari and Nath [19] by two methods, namely, analytically by the homotopy analysis method and numerically by the Keller box method. An unsteady mixed convection boundary layer flow and heat transfer due to a stretching vertical surface with variable fluid properties was presented by Ishak et al. [20]. Mahdy [21] considered the same flow problem for nanofluids. Recently Vajravelu et al. [22] extended the work of Ishak et al. [20] in the presence of thermal radiation, and most recently Mohamed [23] performed a similar work with a variable viscosity and viscous dissipation. In all of these studies, some of the boundary layer flow problems were steady with the species concentrations and fluid properties being assumed to be constant, and some were unsteady and involved variable fluid properties, but the species concentration was not considered.

Thus, the present investigation is focused on an unsteady mixed convection boundary layer flow over a vertically stretching sheet with variable fluid properties in the presence of suction/injection. The boundary layer equations governed by the partial differential equations are transformed into a system of nonlinear ordinary differential equations, which are solved numerically by the Keller box method described in detail in [24, 25].

1. MATHEMATICAL FORMULATION

Let us consider an unsteady mixed convection flow of an incompressible viscous fluid past over a semi-infinite vertically stretching porous sheet. The problem is solved in a Cartesian coordinate system, where the x axis is measured along the sheet in the upward direction and the y axis is measured in the direction normal to the stretching sheet (Fig. 1). At the time $t < 0$, the fluid and heat and mass fluxes are assumed to be steady. The stretching sheet velocity $U_w(x,t)$, its temperature $T_w(x,t)$, and species concentration $C_w(x,t)$ at each time instant t are assumed to be linear functions of x. All thermophysical properties of the sheet and the ambient fluid are assumed to be constant, except for the variable thermal conductivity. The fluid considered here is a medium absorbing and emitting radiation, but not a scattering medium. The boundary layer equations under the Boussinesq approximation have the form

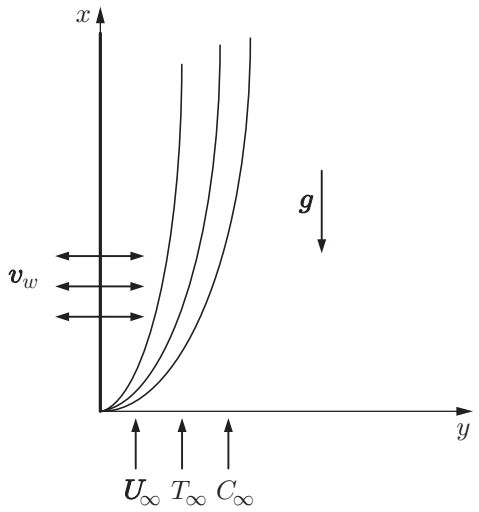

Fig. 1. Physical model and coordinate system.

$$\frac{\partial u}{\partial x}+\frac{\partial v}{\partial y}=0; \tag{1}$$

$$\frac{\partial u}{\partial t}+u\,\frac{\partial u}{\partial x}+v\,\frac{\partial u}{\partial y}=\nu\,\frac{\partial^2 u}{\partial y^2}\pm g\beta_T(T-T_\infty)\pm g\beta_C(C-C_\infty); \tag{2}$$

$$\rho c_p\Big(\frac{\partial T}{\partial t}+u\,\frac{\partial T}{\partial x}+v\,\frac{\partial T}{\partial y}\Big)=\frac{\partial}{\partial y}\Big(K(T)\,\frac{\partial T}{\partial y}\Big)-\frac{\partial q_r}{\partial y}; \tag{3}$$

$$\frac{\partial C}{\partial t}+u\,\frac{\partial C}{\partial x}+v\,\frac{\partial C}{\partial y}=D\,\frac{\partial^2 C}{\partial y^2}, \tag{4}$$

and the boundary conditions are

$$y=0: \qquad u=U_w, \quad v=v_w(t), \quad T=T_w, \quad C=C_w,$$

$$y\to\infty: \qquad u\to 0, \quad T\to T_\infty, \quad C\to C_\infty.$$

Here u and v are the velocity components in the x and y directions, $K(T)=K_\infty(1+\varepsilon(T-T_\infty)/\Delta T)$ is the variable thermal conductivity [13], $\Delta T=T_w-T_\infty$, T_w is the surface temperature, ε is a small parameter, K_∞ is the thermal conductivity of the fluid far away from the sheet, ν is the kinematic viscosity, β_T and β_C are the volumetric coefficients of thermal and concentration expansion, respectively, ρ is the fluid density, c_p is the specific heat, q_r is the radiative heat flux, and D is the mass diffusivity.

The last two terms in Eq. (2) are due to the buoyancy force. The plus and minus signs refer to the buoyancy-assisting and buoyancy-opposing flow situations, respectively.

Following [13, 20, 22], we define

$$U_w(x,t)=\frac{ax}{1-ct}, \qquad T_w(x,t)=T_\infty+\frac{bx}{(1-ct)^2}, \qquad C_w(x,t)=C_\infty+\frac{mx}{(1-ct)^2}$$

(a, b, c, and m are constants). Using the Rosseland approximation [26], we can write the radiative heat flux as

$$q_r=-\frac{4\sigma^*}{3k^*}\,\frac{\partial T^4}{\partial y}, \tag{5}$$

where σ^* and k^* are the Stefan–Boltzmann constant and the mean absorption coefficient, respectively. The temperature difference within the flow region, namely, the term T^4 is assumed to be a linear function of temperature. The linear approximation for temperature is obtained by expanding T^4 into a Taylor series at infinity and neglecting higher-order terms:

$$T^4\simeq 4T_\infty^3T-3T_\infty^4. \tag{6}$$

With the use of the definition of $K(T)$ and in view of Eqs. (5) and (6), Eq. (3) is reduced to

$$\rho c_p\Big(\frac{\partial T}{\partial t}+u\,\frac{\partial T}{\partial x}+v\,\frac{\partial T}{\partial y}\Big)=\frac{\varepsilon k_\infty}{T_w-T_\infty}\Big(\frac{\partial T}{\partial y}\Big)^2+\Big(K(T)+\frac{16\sigma^*T_\infty^3}{3k^*}\Big)\frac{\partial^2 T}{\partial y^2}. \tag{7}$$

The following similarity transformations are introduced:

$$\eta=y\Big(\frac{a}{\nu(1-ct)}\Big)^{1/2}, \quad \psi(x,y,t)=\Big(\frac{\nu a}{1-ct}\Big)^{1/2}xf(\eta), \quad G(\eta)=\frac{T-T_\infty}{T_w-T_\infty},$$

$$H(\eta)=\frac{C-C_\infty}{C_w-C_\infty}, \quad \mathrm{Gr}=\frac{g\beta_T(T_w-T_\infty)L^3}{\nu^2}, \quad \mathrm{Gr}_*=\frac{g\beta_C(C_w-C_\infty)L^3}{\nu^2},$$

$$\lambda=\frac{\mathrm{Gr}}{\mathrm{Re}_L^2}, \quad \lambda_1=\frac{\mathrm{Gr}_*}{\mathrm{Re}_L^2}, \quad \mathrm{Re}_L=\frac{U_wL}{\nu}, \quad \mathrm{Pr}=\frac{\nu}{\alpha_\infty}, \quad \alpha_\infty=\frac{K_\infty}{\rho c_p}.$$

Here $\psi(x,y,t)$ is the stream function ($u=\partial\psi/\partial y$ and $v=-\partial\psi/\partial x$), Gr and Gr_* are the Grashof numbers due to temperature and concentration, respectively, L is the sheet length, λ and λ_1 are the buoyancy forces due to temperature and concentration gradients, respectively, U_w is the stretching sheet velocity, and α_∞ is the thermal

diffusivity. Using the above-described transformations and the definition of $K(T)$, we convert Eqs. (2), (7), and (4) to the coupled nonlinear ordinary differential equations

$$f''' + ff'' - f'^2 - M(f' + \eta f''/2) + \lambda(G + NH) = 0,$$

$$((1 + \varepsilon G + N_r)G')' - \Pr\,(f'G - G'f) - M\Pr\,(2G + \eta G'/2) = 0, \tag{8}$$

$$H'' - \mathrm{Sc}\,(f'H - H'f) - M\mathrm{Sc}\,(2H + \eta H'/2) = 0$$

with the boundary conditions

$$\eta \to \infty: \qquad f(0) = s, \quad f'(0) = 1, \quad G(0) = 1, \quad H(0) = 1, \quad f' \to 0, \quad G \to 0, \quad H \to 0, \tag{9}$$

where the prime denotes differentiation with respect to η, $M = c/a$ is the unsteady parameter, $N_r = 16\sigma^* T_\infty/(3K_\infty k^*)$ is the radiation parameter, $s = -v_0/\sqrt{(1 - ct)/(\nu a)}$ is the suction/injection parameter ($s < 0$, $s > 0$, and $s = 0$ correspond to injection, suction, and impermeability, respectively), and $N = \lambda_1/\lambda$ is the ratio of buoyancy forces ($N = 0$ indicates that there is no buoyancy force effect due to mass diffusion and $N = \infty$ corresponds to the absence of the buoyancy effect due to thermal diffusion).

The physical quantities of interest from the engineering point of view are the local skin friction coefficient

$$C_f = 2\tau_w/(\rho u_w^2), \tag{10}$$

the local Nusselt number

$$\mathrm{Nu}_x = xq_w/(k_\infty(T_w - T_\infty)), \tag{11}$$

and the local Sherwood number

$$\mathrm{Sh}_x = xq_m/(D(C_w - C_\infty)). \tag{12}$$

($\tau_w = \mu\,\partial u/\partial y|_{y=0}$ is the surface shear stress, $q_w = -k_\infty\,\partial T/\partial y|_{y=0}$ is the wall heat flux, $q_m = -k_\infty\,\partial T/\partial y|_{y=0}$ is the mass flux, and μ is the dynamic viscosity).

With the use of the similarity variables, Eqs. (10)–(12) are written as

$$C_f\sqrt{\mathrm{Re}_x}/2 = f''(0), \qquad \mathrm{Nu}_x/\sqrt{\mathrm{Re}_x} = -G'(0), \qquad \mathrm{Sh}_x/\sqrt{\mathrm{Re}_x} = -H'(0),$$

where $\mathrm{Re}_x = U_w x/\nu$ is the local Reynolds number.

2. METHOD OF THE SOLUTION

The system of nonlinear ordinary differential equations (8) with the boundary condition (9) was solved numerically by the Keller box method [24, 25], which is implemented in the Matlab software package. The Keller box method is an implicit finite difference method that can be used to solve differential equations.

Introducing new variables $u(x, \eta)$, $v(x, \eta)$, $p(x, \eta)$, and $q(x, \eta)$ with

$$f' = u, \quad u' = v, \quad G' = p, \quad H' = q,$$

we can write Eqs. (8) as

$$v' + fv - u^2 - M(u + \eta v/2) + \lambda(G + NH) = 0,$$

$$(1 + N_r + \varepsilon G)p' + \varepsilon p^2 - \Pr\,(uG - pf) - M\Pr\,(2G + \eta p/2) = 0,$$

$$q' - \mathrm{Sc}(uH - qf) - M\mathrm{Sc}\,(2H + \eta q/2) = 0.$$

We now consider the net rectangle in the plane (x, η):

$$x^0 = 0, \qquad x^n = x^{n-1} + k_n, \quad n = 1, 2, \ldots, N,$$

$$\eta_0 = 0, \qquad \eta_j = \eta_{j-1} + h_j, \quad j = 1, 2, \ldots, J$$

(k_n is the x-spacing and h_j is the η-spacing between the nodes). We start writing the finite difference equations for the node $(x^n, \eta_{j-1/2})$ by using the central differences:

$$(f_j - f_{j-1})h_j^{-1} = u_{j-1/2}, \qquad (u_j - u_{j-1})h_j^{-1} = v_{j-1/2},$$

$$(G_j - G_{j-1})h_j^{-1} = p_{j-1/2}, \qquad (H_j - H_{j-1})h_j^{-1} = q_{j-1/2},$$

$$(v_j - v_{j-1})h_j^{-1} + f_{j-1/2}v_{j-1/2} - (u_{j-1/2})^2 - M(u_{j-1/2} + \eta_j v_{j-1/2}/2)$$

$$- \lambda(G_{j-1/2} + NH_{j-1/2}) = 0, \tag{13}$$

$$(1 + N_r + \varepsilon G_{j-1/2})(p_j - p_{j-1})h_j^{-1} + \varepsilon(p_{j-1/2})^2 - \mathrm{Pr}\,(u_{j-1/2}G_{j-1/2} - p_{j-1/2}f_{j-1/2})$$

$$- M\mathrm{Pr}\,(2G_{j-1/2} + \eta_j p_{j-1/2}/2) = 0,$$

$$(q_j - q_{j-1})h_j^{-1} - \mathrm{Sc}\,(u_{j-1/2}H_{j-1/2} - q_{j-1/2}f_{j-1/2}) - M\mathrm{Sc}\,(2H_{j-1/2} + \eta_j q_{j-1/2}/2) = 0.$$

Here $u_{j-1/2} = (u_j + u_{j-1})/2$, etc. Equations (13) are nonlinear algebraic equations and, therefore, have to be linearized before the factorization scheme can be used. Let us write the Newton iterative scheme. For the $(i+1)$th iteration, we have

$$f_j^{i+1} = f_j^i + \delta f_j^i, \tag{14}$$

where f is an arbitrary dependent variable. By substituting expressions (14) into Eqs. (13) and dropping the quadratic and higher-order terms in δf_j^{i+1}, we obtain a tridiagonal system of algebraic equations

$$\delta f_j - \delta f_{j-1} - h_j(\delta u_j + \delta u_{j-1})/2 = (r_1)_{j-1/2},$$

$$\delta u_j - \delta u_{j-1} - h_j(\delta v_j + \delta v_{j-1})/2 = (r_2)_{j-1/2},$$

$$\delta G_j - \delta G_{j-1} - h_j(\delta p_j + \delta p_{j-1})/2 = (r_3)_{j-1/2},$$

$$\delta H_j - \delta H_{j-1} - h_j(\delta q_j + \delta q_{j-1})/2 = (r_4)_{j-1/2},$$

$$(a_1)_j\,\delta v_j + (a_2)_j\,\delta v_{j-1} + (a_3)_j\,\delta f_j + (a_4)_j\,\delta f_{j-1} + (a_5)_j\,\delta u_j + (a_6)_j\,\delta u_{j-1}$$

$$+ (a_7)_j\,\delta G_j + (a_8)_j\,\delta G_{j-1} + (a_9)_j\,\delta H_j + (a_{10})_j\,\delta H_{j-1} = (r_5)_{j-1/2},$$

$$(b_1)_j\,\delta p_j + (b_2)_j\,\delta p_{j-1} + (b_3)_j\,\delta G_j + (b_4)_j\,\delta G_{j-1} + (b_5)_j\,\delta u_j + (b_6)_j\,\delta u_{j-1}$$

$$+ (b_7)_j\,\delta f_j + (b_8)_j\,\delta f_{j-1} = (r_6)_{j-1/2},$$

$$(c_1)_j\,\delta q_j + (c_2)_j\,\delta q_{j-1} + (c_3)_j\,\delta u_j + (c_4)_j\,\delta u_{j-1} + (c_5)_j\,\delta H_j + (c_6)_j\,\delta H_{j-1}$$

$$+ (c_7)_j\,\delta f_j + (c_8)_j\,\delta f_{j-1} = (r_7)_{j-1/2},$$

where

$$(a_1)_j = 1 + h_j(f_j + f_{j-1})/4 - Mh_j\eta_j/4, \qquad (a_2)_j = -1 + h_j(f_j + f_{j-1})/4 - Mh_j\eta_j/4,$$

$$(a_3)_j = (a_4)_j, \qquad (a_4)_j = h_j(v_j + v_{j-1})/4, \qquad (a_5)_j = (a_6)_j,$$

$$(a_6)_j = -h_j(u_j + u_{j-1})/2 - Mh_j/2, \qquad (a_7)_j = (a_8)_j, \qquad (a_8)_j = \lambda h_j/2,$$

$$(a_9)_j = (a_{10})_j, \qquad (a_{10})_j = N\lambda h_j/2,$$

$$(b_1)_j = 1 + \frac{\varepsilon}{2(1+N_r)}\,(G_j + G_{j-1}) + \frac{\varepsilon h_j}{2(1+N_r)}\,(p_j + p_{j-1}) + \frac{\mathrm{Pr}\,h_j}{4(1+N_r)}\,(f_j + f_{j-1}) - \frac{\mathrm{Pr}\,\eta_j h_j}{4(1+N_r)},$$

$$(b_2)_j = -1 - \frac{\varepsilon}{2(1+N_r)}\,(G_j + G_{j-1}) + \frac{\varepsilon h_j}{2(1+N_r)}\,(p_j + p_{j-1}) + \frac{\mathrm{Pr}\,h_j}{4(1+N_r)}\,(f_j + f_{j-1}) - \frac{\mathrm{Pr}\,\eta_j h_j}{4(1+N_r)},$$

$$(b_3)_j = (b_4)_j = \frac{\varepsilon}{2(1+N_r)}\,(p_j - p_{j-1}) - \frac{\Pr h_j}{4(1+N_r)}\,(u_j + u_{j-1}) - \frac{\Pr h_j}{1+N_r},$$

$$(b_5)_j = (b_6)_j = -\frac{\Pr h_j}{4(1+N_r)}\,(G_j + G_{j-1}), \qquad (b_7)_j = (b_8)_j = \frac{\Pr h_j}{4(1+N_r)}\,(p_j + p_{j-1}),$$

$$(c_1)_j = 1 + \mathrm{Sc}\,(f_j + f_{j-1})/4 - M\mathrm{Sc}\eta_j h_j/4, \qquad (c_2)_j = -1 + \mathrm{Sc}\,(f_j + f_{j-1})/4 - M\mathrm{Sc}\eta_j h_j/4,$$

$$(c_3)_j = (c_4)_j = -\mathrm{Sc}h_j(H_j + H_{j-1})/4, \qquad (c_5)_j = (c_6)_j = -\mathrm{Sc}h_j(u_j + u_{j-1})/4 - M\mathrm{Sc}h_j,$$

$$(c_7)_j = (c_8)_j = \mathrm{Sc}h_j(q_j + q_{j-1})/4,$$

$$(r_1)_j = f_{j-1} - f_j + h_j(u_j + u_{j-1})/2, \qquad (r_2)_j = u_{j-1} - u_j + h_j(v_j + v_{j-1})/2,$$

$$(r_3)_j = G_{j-1} - G_j + h_j(p_j + p_{j-1})/2, \qquad (r_4)_j = H_{j-1} - H_j + h_j(q_j + q_{j-1})/2,$$

$$(r_5)_j = v_{j-1} - v_j - h_j(f_j + f_{j-1})(v_j + v_{j-1})/4 + h_j(u_j + u_{j-1})^2/4 + Mh_j(u_j + u_{j-1})/2$$
$$+ Mh_j\eta_j(v_j + v_{j-1})/4 - \lambda h_j(G_j + G_{j-1})/2 - \lambda N h_j(H_j + H_{j-1})/2,$$

$$(r_6)_j = p_{j-1} - p_j - \frac{\varepsilon}{2(1+N_r)}\,(G_j + G_{j-1})(p_j - p_{j-1}) - \frac{\varepsilon h_j}{4(1+N_r)}\,(p_j + p_{j-1})^2$$
$$+ \frac{\Pr h_j}{4(1+N_r)}\,(u_j + u_{j-1})(G_j + G_{j-1}) - \frac{\Pr h_j}{4(1+N_r)}\,(f_j + f_{j-1})(p_j + p_{j-1})$$
$$+ \frac{M\Pr h_j}{1+N_r}\,(G_j + G_{j-1}) + \frac{M\Pr \eta_j h_j}{4(1+N_r)}\,(p_j + p_{j-1}),$$

$$(r_7)_j = q_{j-1} - q_j + \mathrm{Sc}h_j(u_j + u_{j-1})(H_j + H_{j-1})/4 - \mathrm{Sc}h_j(f_j + f_{j-1})(q_j + q_{j-1})/4$$
$$+ M\mathrm{Sc}h_j(H_j + H_{j-1}) + M\mathrm{Sc}h_j\eta_j(q_j + q_{j-1})/4.$$

Linearizing the boundary conditions, we obtain

$$\delta f_0 = s, \quad \delta u_0 = 1, \quad \delta G_0 = 1, \quad \delta H_0 = 1, \quad \delta u_J = 0, \quad \delta G_J = 0, \quad \delta H_J = 0.$$

Hence, the linearized system can be written in the matrix form as

$$A\delta = r, \tag{15}$$

where

$$A = \begin{bmatrix} [A_1] & [C_1] & & & & & & \\ [B_2] & [A_2] & [C_2] & & & & & \\ & \cdot & \cdot & \cdot & & & & \\ & & \cdot & \cdot & \cdot & & & \\ & & & \cdot & \cdot & \cdot & & \\ & & & & [B_{J-1}] & [A_{J-1}] & [C_{J-1}] & \\ & & & & & [B_J] & [A_J] & \end{bmatrix}, \quad \delta = \begin{bmatrix} \delta_1 \\ \delta_2 \\ \cdot \\ \cdot \\ \cdot \\ \delta_{J-1} \\ \delta_J \end{bmatrix}, \quad r = \begin{bmatrix} r_1 \\ r_2 \\ \cdot \\ \cdot \\ \cdot \\ r_{J-1} \\ r_J \end{bmatrix}.$$

The elements of the matrix A are

$$[A_1] = \begin{bmatrix} 0 & 0 & 0 & 1 & 0 & 0 & 0 \\ -d_1 & 0 & 0 & 0 & -d_1 & 0 & 0 \\ 0 & -d_1 & 0 & 0 & 0 & -d_1 & 0 \\ 0 & 0 & -d_1 & 0 & 0 & 0 & -d_1 \\ a_2 & 0 & 0 & a_3 & a_1 & 0 & 0 \\ 0 & b_2 & 0 & b_7 & 0 & b_1 & 0 \\ 0 & 0 & c_2 & c_7 & 0 & 0 & c_1 \end{bmatrix}, \qquad d_j = \frac{1}{2}\,h_j,$$

$$[A_j] = \begin{bmatrix} -d_j & 0 & 0 & 1 & 0 & 0 & 0 \\ -1 & 0 & 0 & 0 & -d_j & 0 & 0 \\ 0 & -1 & 0 & 0 & 0 & -d_j & 0 \\ 0 & 0 & -1 & 0 & 0 & 0 & -d_j \\ (a_6)_j & (a_8)_j & (a_{10})_j & (a_3)_j & (a_1)_j & 0 & 0 \\ (b_6)_j & (b_4)_j & 0 & (b_7)_j & 0 & (b_1)_j & 0 \\ (c_4)_j & 0 & (c_6)_j & (c_7)_j & 0 & 0 & (c_1)_j \end{bmatrix}, \qquad 2 \leqslant j \leqslant J,$$

$$[B_j] = \begin{bmatrix} 0 & 0 & 0 & -1 & 0 & 0 & 0 \\ 0 & 0 & 0 & 0 & -d_j & 0 & 0 \\ 0 & 0 & 0 & 0 & 0 & -d_j & 0 \\ 0 & 0 & 0 & 0 & 0 & 0 & -d_j \\ 0 & 0 & 0 & (a_4)_j & (a_2)_j & 0 & 0 \\ 0 & 0 & 0 & (b_8)_j & 0 & (b_2)_j & 0 \\ 0 & 0 & 0 & (c_8)_j & 0 & 0 & (c_2)_j \end{bmatrix}, \qquad 2 \leqslant j \leqslant J,$$

$$[C_j] = \begin{bmatrix} -d_j & 0 & 0 & 0 & 0 & 0 & 0 \\ 1 & 0 & 0 & 0 & 0 & 0 & 0 \\ 0 & 1 & 0 & 0 & 0 & 0 & 0 \\ 0 & 0 & 1 & 0 & 0 & 0 & 0 \\ (a_5)_j & (a_7)_j & (a_9)_j & 0 & 0 & 0 & 0 \\ (b_5)_j & (b_3)_j & 0 & 0 & 0 & 0 & 0 \\ (c_3)_j & 0 & (c_5)_j & 0 & 0 & 0 & 0 \end{bmatrix}, \qquad 1 \leqslant j \leqslant J-1,$$

$$\delta_1 = \begin{bmatrix} \delta v_0 \\ \delta p_0 \\ \delta q_0 \\ \delta f_1 \\ \delta v_1 \\ \delta p_1 \\ \delta q_1 \end{bmatrix}, \qquad \delta_j = \begin{bmatrix} \delta u_{j-1} \\ \delta G_{j-1} \\ \delta H_{j-1} \\ \delta f_j \\ \delta v_j \\ \delta p_j \\ \delta q_j \end{bmatrix}, \quad 2 \leqslant j \leqslant J, \qquad r_j = \begin{bmatrix} (r_1)_{j-1/2} \\ (r_2)_{j-1/2} \\ (r_3)_{j-1/2} \\ (r_4)_{j-1/2} \\ (r_5)_{j-1/2} \\ (r_6)_{j-1/2} \\ (r_7)_{j-1/2} \end{bmatrix}, \quad 1 \leqslant j \leqslant J.$$

To solve Eq. (15), we assume that the matrix A is non-singular and it can be factored into

$$A = LU, \tag{16}$$

where

$$L = \begin{bmatrix} [\alpha_1] & & & & & \\ [\beta_2] & [\alpha_2] & & & & \\ & \cdot & \cdot & \cdot & & \\ & & & [\alpha_{J-1}] & & \\ & & & [\beta_2] & [\alpha_J] \end{bmatrix}, \qquad U = \begin{bmatrix} [I] & [\Gamma_1] & & & & \\ & [I] & [\Gamma_2] & & & \\ & & \cdot & \cdot & \cdot & \\ & & & & [I] & [\Gamma_{J-1}] \\ & & & & & [I] \end{bmatrix},$$

$[I]$ is the unit matrix of order 7×7, and $[\alpha_i]$ and $[\Gamma_i]$ are 7×7 matrices whose elements are determined from the following equations:

$$[\alpha_1] = [A_1], \quad [A_1][\Gamma_1] = [C_1], \quad [\alpha_j] = [A_j] - [B_j][\Gamma_{j-1}],\ j = 2, 3, 4, \ldots, J.$$

Substitution of Eq. (16) into Eq. (15) yields

$$LU\delta = r. \tag{17}$$

If we define

$$U\delta = W,$$

Table 1. Values of $-G'(0)$ obtained by different researchers

M	λ	Pr	Data [14]	Data [15]	Data [20]	Data [22]	Present data
0	0	0.72	0.8086	0.8058	0.8086	0.808 636	0.808 637
0	0	1.00	1.0000	0.9610	1.0000	1.000 000	1.000 000
0	0	3.00	1.9237	1.9144	1.9237	1.923 687	1.923 691
0	0	10.00	3.7207	3.7006	3.7207	3.720 788	3.720 791
0	0	100.00	12.2940	—	12.2941	12.300 390	12.300 395
1	0	1.00	—	—	1.6820	1.681 921	1.680 799
1	1	1.00	—	—	1.7039	1.703 910	1.702 720
1	1	1.00	—	—	1.0873	1.087 206	1.087 279
0	2	1.00	—	—	1.4230	1.422 980	1.142 341
0	3	1.00	—	—	1.1853	1.185 197	1.185 293

Eq. (17) becomes

$$LW = r, \tag{18}$$

where $W = [W_1, W_2, W_3, W_4, W_5, W_6, W_7]^{\mathrm{t}}$; W_j are the 7×1 column matrices. The elements of W can be found by solving Eq. (18):

$$[\alpha_1][W_1] = [r_1], \qquad [\alpha_j][W_j] = [r_j] - [\beta_j][W_{j-1}], \quad j = 2, 3, 4, \ldots, J.$$

Once the elements of W are found, we can find the solution of Eq. (18) using the recurrent relations

$$[\delta_J] = [W_J], \qquad [\delta_j] = [W_j] - [\Gamma_j][\delta_{j+1}], \quad 1 \leqslant j \leqslant j - 1.$$

The calculations are repeated until the convergence criterion $|\delta v_0^i| \leqslant \varepsilon_1$ (ε_1 is a small positive number prescribed) is satisfied.

3. RESULTS AND DISCUSSION

The computation were performed for different values of the Prandtl number Pr , Schmidt number Sc, buoyancy force parameter due to the temperature gradient λ, unsteady parameter M, variable thermal conductivity parameter ε, radiation parameter N_r, buoyancy force ratio parameter N, and suction/injection parameter s. The surface heat transfer rate $-G'(0)$ obtained in the present study by the above-described algorithm is in good agreement with the values obtained in [14, 15, 20, 22] (Table 1).

Figure 2a shows the velocity distributions f' over the spatial coordinate η for different values of the parameter λ in the cases of injection ($s < 0$), impermeability ($s = 0$), and suction ($s > 0$) for steady and unsteady flows. As we observe from Fig. 2a, an increase in the buoyancy force parameter λ leads to an increase in the fluid velocity. A velocity overshoot is observed near the surface; then the velocity decreases and tends to zero as $\eta \to \infty$. The fluid velocity is higher in the case of injection than that in the case of suction. Furthermore, the fluid velocity is greater in the steady case than that in the unsteady flow.

Figure 2b shows the temperature distributions over the spatial coordinate η for the same values of the problem parameters as in Fig. 2a. It is seen that an increase in the buoyancy force parameter λ results in a decrease in the fluid temperature in all cases (injection, impermeability, and suction). The thermal boundary layer is thicker in the case of injection than that in the case of suction. The temperature in the steady case is higher than that in the unsteady flow.

An increase in the buoyancy force ratio parameter N leads to an increase in the fluid velocity in all of the circumstances: injection, impermeability, and suction (Fig. 3). The fluid velocity is higher in the steady case than that in the unsteady case. In the assisting flow ($N > 0$), the solution of the momentum equation exists for large values of N; however, in the opposing flow ($N < 0$), the solution exists for small values of N.

Figure 4 shows the temperature distributions over the spatial coordinate η for different values of the parameter ε for the steady and unsteady flows in the cases of injection, impermeability, and suction. It is seen that there is a minor increase in the fluid temperature with increasing ε in all three cases. The fluid temperature in the steady case is again greater than that in the unsteady case.

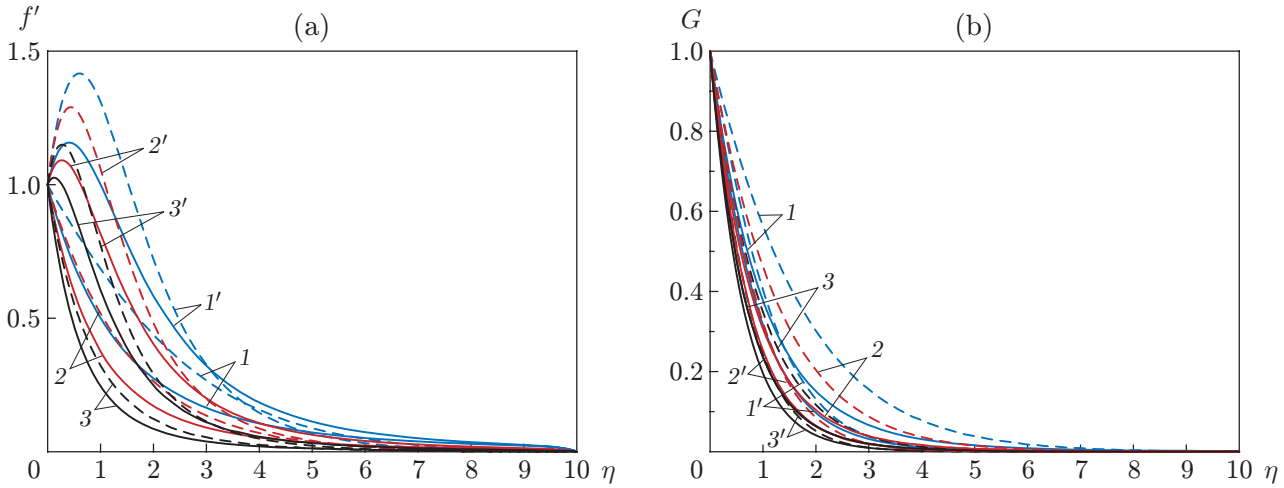

Fig. 2. Velocity (a) and temperature (b) profiles versus the spatial coordinate η for $N = \varepsilon = N_r = 0.2$, Pr $= 0.7$, and different values of λ, s, and M: the solid and dashed curves refer to $M = 1$ and $M = 0$, respectively; $\lambda = 0.5$ (*1–3*) and 5 (*1′–3′*); $s = -1$ (*1 and 1′*), 0 (*2 and 2′*), and 1 (*3 and 3′*).

Table 2. Skin friction coefficient $f''(0)$, heat transfer rate $-G'(0)$, and mass transfer rate $-H'(0)$ on the sheet surface for $s = 0$, $\varepsilon = 0.1$, and $N_r = 0.1$

λ	N	Pr	Sc	M	$f''(0)$	$-G'(0)$	$-H'(0)$
0.1	1.00	0.7	0.23	0	−0.858 408	0.768 940	0.406 118
0.1	1.00	1.0	0.23	0	−0.865 023	0.953 517	0.403 615
0.1	1.00	7.0	0.23	0	−0.890 728	2.844 145	0.398 804
0.1	1.00	0.7	0.23	0	−1.235 140	1.290 678	0.773 027
0.1	1.00	1.0	0.23	1	−1.238 657	1.557 566	0.772 696
0.1	1.00	7.0	0.23	1	−1.255 358	4.276 605	0.771 587
0.1	−0.01	7.0	0.23	1	−0.729 728	0.784 582	0.410 264
0.1	0	0.7	0.23	0	−0.726 130	0.785 696	0.411 591
0.5	1.00	0.7	0.23	0	−0.414 382	0.852 052	0.475 624
0.5	10.00	0.7	0.23	0	0.059 986	0.015 111	0.010 195
0.5	−0.01	0.7	0.23	0	−1.136 448	1.296 389	0.777 035
0.5	0	0.7	0.23	1	−1.134 162	1.296 559	0.777 170
0.5	1.00	0.7	0.23	1	−0.910 271	1.312 644	0.789 867
0.5	10.00	0.7	0.23	1	0.860 174	1.416 167	0.867 530
0.5	10.00	0.7	0.23	1	−0.562 480	0.824 953	0.451 661
0.5	0.50	0.7	0.94	0	−0.620 637	0.800 854	1.047 223
0.5	0.50	0.7	2.56	0	−0.651 321	0.793 737	1.832 906
0.5	0.50	0.7	10.00	0	−0.676 175	0.793 609	3.772 886
0.5	0.50	0.7	0.23	0	−1.021 099	1.304 807	0.783 711
0.5	0.50	0.7	0.94	1	−1.053 660	1.301 129	1.646 042
0.5	0.50	0.7	2.56	1	−1.075 946	1.299 083	2.771 281
0.5	0.50	0.7	10.00	1	−1.099 863	1.297 477	5.572 851

Figure 5 shows the temperature distributions over the spatial coordinate η for different values of the radiation parameter N_r. The figure tells us that the fluid temperature increases in all three cases (injection, impermeability, and suction) as the radiation parameter increases. In a similar way, as we discussed above, the steady state temperature is higher than that in the unsteady case.

Figure 6 shows the skin friction coefficient as a function of the parameter λ for different values of M. It is seen that the skin friction coefficient increases with decreasing M and increasing λ. It is also evident from the figure that the skin friction coefficient is higher in the case of injection than that in the case of suction. The values of the skin friction coefficient $f''(0)$, heat transfer rate $-G'(0)$, and mass transfer rate $-H'(0)$ in the impermeable case are listed in Table 2 for different values of the problem parameters. It is observed from Table 2 that the skin

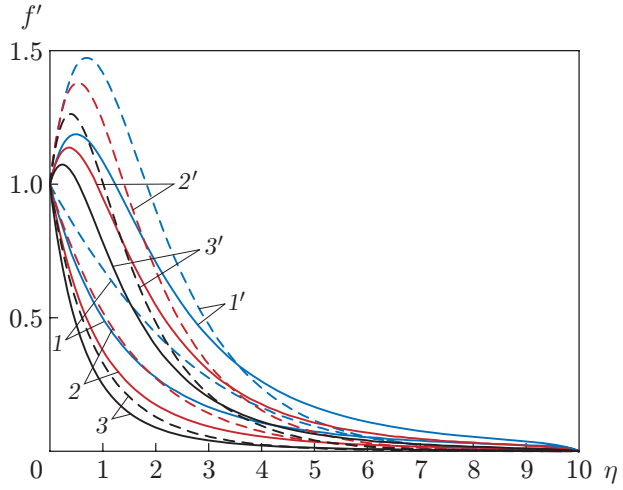

Fig. 3.

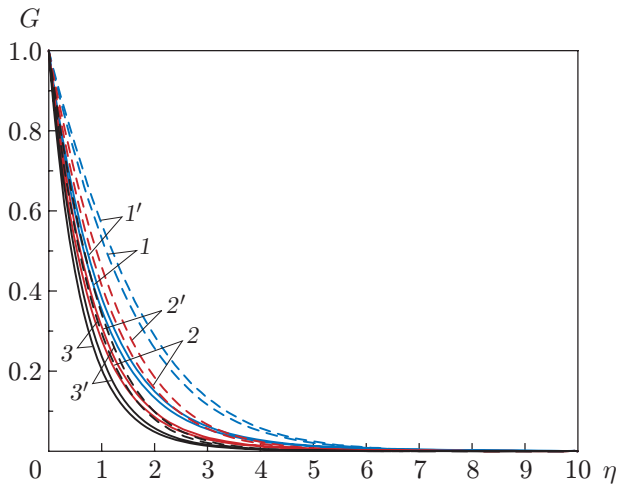

Fig. 4.

Fig. 3. Velocity profiles versus the spatial coordinate η for $\lambda = \varepsilon = N_r = 0.5$ and different values of N, s, and M: $N = 0.5$ (*1–3*) and 5 (*1′–3′*); other notations the same as in Fig. 2.

Fig. 4. Temperature profiles versus the spatial coordinate η for $\lambda = N = N_r = 0.5$, Pr $= 1$, and different values of ε, s, and M: $\varepsilon = 0.25$ (*1–3*) and 1 (*1′–3′*); other notations the same as in Fig. 2.

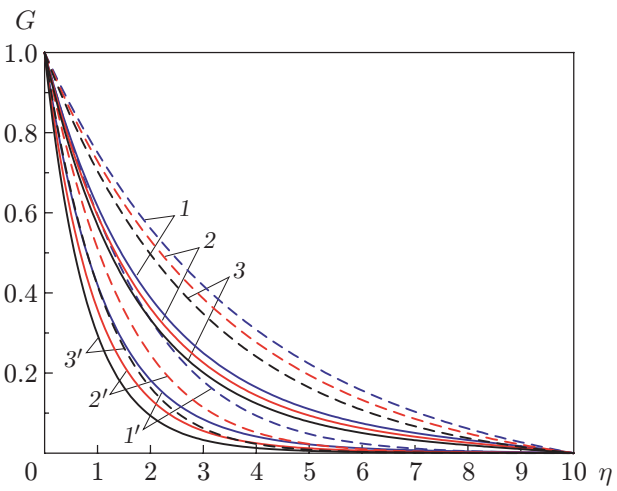

Fig. 5.

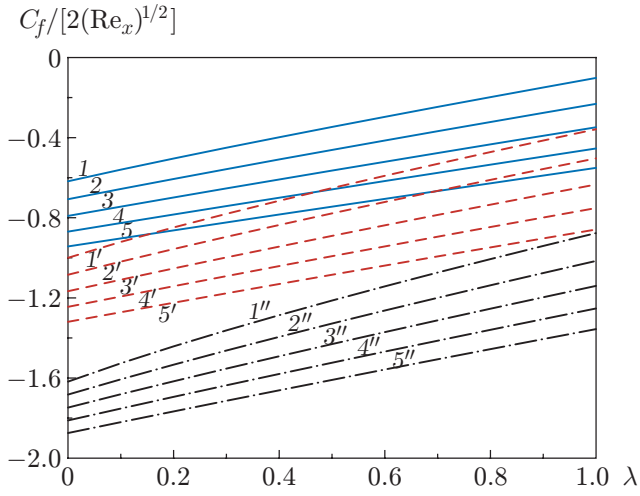

Fig. 6.

Fig. 5. Temperature profiles versus the spatial coordinate η for $\lambda = N = \varepsilon = 0.5$, Pr $= 0.7$, and different values of N_r, s, and M: $N_r = 0.5$ (*1–3*) and 5 (*1′–3′*); other notations the same as in Fig. 2.

Fig. 6. Skin friction coefficients versus the parameter λ for $N = N_r = 0.2$, Pr $= 0.7$, Sc $= 0.23$, $\varepsilon = 0.1$, and different values of s and M: $s = -1$ (solid curves), 0 (dashed curves), and 1 (dot-and-dashed curves); $M = 0$ (*1*, *1′*, and *1″*), 0.25 (*2*, *2′*, and *2″*), 0.5 (*3*, *3′*, and *3″*), 0.75 (*4*, *4′*, and *4″*), and 1 (*5*, *5′*, and *5″*).

friction coefficient decreases with increasing buoyancy force ratio parameter N, the heat transfer rate increases with increasing Prandtl number, and the mass transfer rate increases with increasing Schmidt number.

CONCLUSIONS

The problem of an unsteady double diffusive mixed convection boundary layer flow of a viscous incompressible fluid flowing over a vertically stretching sheet is solved by the Keller box method. The problem is considered with allowance for thermal radiation in situations with suction, impermeability, and injection.

In both steady and unsteady cases, we found that the fluid temperature increases with increasing radiation parameter N_r and decreases with increasing buoyancy force parameter λ. In the case of injection, the fluid velocity is higher than that in the case of suction. The fluid temperature increases with increasing thermal conductivity parameter ϵ. The skin friction coefficient increases with decreasing M and increasing buoyancy force parameter λ. The skin friction coefficient is greater in the case of injection than that in the case of suction.

REFERENCES

1. P. M. Patil, E. Momoniat, and S. Roy, "Influence of Convective Boundary Condition on Double Diffusive Mixed Convection from a Ppermeable Vertical Surface," Int. J. Heat Mass Transfer **70**, 313–321 (2014).
2. H. Blasius, "Grenzschichten in Flussigkeiten Mit Kleiner Reibung," Z. Angew Math. Phys. **56**, 1–37 (1908).
3. B. C. Sakiadis, "Boundary Layer Behavior on Continuous Solid Surface: the Boundary Layer on a Continuous Flat Surface," AIChE J. **7**, 221–225 (1961).
4. B. Cortell, "Radiation Effects in the Blasius Flow," Appl. Math. Comput. **198**, 333–338 (2008).
5. R. Cortell, "Radiation Effects for the Blasius and Sakiadis Flows with a Convective Surface Boundary Condition," Appl. Math. Comput. **206**, 832–840 (2008).
6. P. M. Patil, S. Roy, and A. J. Chamkha, "Double Diffusive Mixed Convection Flow over a Moving Vertical Plate in the Presence of Internal Heat Generation and a Chemical Reaction," Turkish J. Eng. Environ Sci. **33**, 193–205 (2009).
7. O. Aydn and A. Kaya, "Laminar Boundary Layer Flow over a Horizontal Permeable Flat Plate," Appl. Math. Comput. **161**, 229–240 (2005).
8. N. Ahmad, Z. U. Siddiqui, and M. K.Mishra, "Boundary Layer Flow and Heat Transfer Past a Stretching Plate with Variable Thermal Conductivity," Int. J. Non-Linear Mech. **45**, 306–309 (2010).
9. K. Bhattacharyya, S. Mukhopadhyay, and G. C. Layek, "Similarity Solution of Mixed Convective Boundary Layer Slip Flow over a Vertical Plate," Ain Shams Eng. J. **4**, 299–305 (2013).
10. O. Aydn and A. Kaya, "MHD Mixed Convection of a Viscous Dissipating Fluid about a Permeable Vertical Flat Platem" Math. Model. **33**, 4086–4096 (2009).
11. I. Pop and T. Na, "A Note on MHD Flow over a Stretching Permeable Surface," Mech. Res. Comm. **25**, 263–269 (1998).
12. N. Bakar, W. Zaimi, R. Hamid, et al., "Boundary Layer Flow over a Stretching Sheet with a Convective Boundary Condition and Slip Effect," World Appl. Sci. J. **17**, 49–53 (2012).
13. T. C. Chiam, "Heat Transfer in a Fluid with Variable Thermal Conductivity over a Linearly Stretching Sheet," Acta Mech. **129**, 63–72 (1998).
14. L. G. Grubka and K. M. Bobba, "Heat Transfer Characteristics of a Continuous Stretching Surface with Variable Temperature," Trans. ASME, J. Heat Transfer **107**, 248–250 (1985).
15. F. M. Ali, R. Nazar, N. M. Arifin, and I. Pop, "Mixed Convection Stagnation-Point Flow on Vertical Stretching Sheet with External Magnetic Field," Appl. Math. Mech. (English ed.) **35**, 155–166 (2014).
16. M. Kumari, A. Slaouti, H. S. Taldlar, et al., "Unsteady Free Convection Flow over a Continuous Moving Vertical Surface," Acta Mech. **116**, 75–82 (1996).
17. A. Ishak, R. Nazar, and I. Pop, "Unsteady Mixed Convection Boundary Layer Flow due to a Stretching Vertical Surface," Arabian J. Sci. Eng. **31** (2B), 165–182 (2006).
18. D. Anilkumar, "Nonsimilar Solutions for Unsteady Mixed Convection from a Moving Vertical Plate," Comm. Nonlinear Sci. Numer. Simulat. **16**, 3147–3157 (2011).

19. M. Kumari and G. Nath, "Unsteady MHD Mixed Convection Flow over an Impulsively Stretched Permeable Vertical Surface in a Quiescent Fluid," Int. J. Non-Linear Mech. **45**, 310–319 (2010).
20. A. Ishak, R. Nazar, and I. Pop, "Boundary Layer Flow and Heat Transfer over an Unsteady Stretching Vertical Surface," Meccanica **44**, 369–375 (2009).
21. A. Mahdy, "Unsteady Mixed Convection Boundary Layer Flow and Heat Transfer of Nanofluids due to Stretching Sheet," Nuclear Eng. Design **249**, 248–255 (2012).
22. K. Vajravelu, K. V. Prasad, and Chiu-On Ng, "Unsteady Convective Boundary Layer Flow of a Viscous Fluid at a Vertical Surface with Variable Fluid Properties," Nonlinear Anal.: Real World Appl. **14**, 455–464 (2013).
23. A. E. Mohamed, "Unsteady Mixed Convection Heat Transfer Along a Vertical Stretching Surface with Variable Viscosity and Viscous Dissipation," J. Egyptian Math. Soc. **22** (3), 529–537 (2014).
24. T. Cebeci, *Physical and Computational Aspects of Convective Heat Transfer*, Ed. by T. Cebeci and P. Bradshaw (Springer-Verlag, New York, 1984).
25. T. Y. Na, *Computational Methods in Engineering Boundary Value Problems* (Academic Press, New York, 1979). (Math. Sci. Eng.; Vol. 145).
26. R. Cortell, "A Numerical Tackling on Sakiadis Flow with Thermal Radiation," Chin. Phys. Lett. **25**, 1340–1342 (2008).